ResearchGate

See discussions, stats, and author profiles for this publication at: https://www.researchgate.net/publication/279585868

A 3D hypoelastic concrete constitutive relationship

Article *in* Journal of the Engineering Mechanics Division · August 1979

CITATIONS
165

READS
644

2 authors, including:

A. E. Elwi
University of Alberta

76 PUBLICATIONS **1,787** CITATIONS

SEE PROFILE

Some of the authors of this publication are also working on these related projects:

Project Bond length of CFP on concrete surfaces View project

All content following this page was uploaded by A. E. Elwi on 08 May 2019.

The user has requested enhancement of the downloaded file.

AUGUST 1979 EM4

14746

JOURNAL OF
THE ENGINEERING
MECHANICS DIVISION

A 3D Hypoelastic Concrete Constitutive Relationship

By Alaa A. Elwi[1] and David W. Murray,[2] M. ASCE

Introduction

In nonlinear finite element analysis of reinforced concrete structures it is necessary to incorporate a multiaxial relationship between stress and strain. Unfortunately this relationship must necessarily be complex if it is to simulate the nonlinear behavior to be expected in real structures. While uniaxial testing is relatively easy to carry out, tests involving biaxial and triaxial response are difficult and there is a scarcity of reliable data upon which to base analytical models. Generally, in literature that attempts to define the failure surface, there is a lack of adequate strain data since these data must be confined to the ascending branch of the stress-strain curves because of the instability attained in tests near peak strengths. Yet it is well known that concrete retains a capacity to resist stress when strained beyond the ultimate strength condition.

This paper is an attempt to develop a nonlinear three-dimensional (axisymmetric) stress-strain relationship for concrete, which incorporates the equivalent uniaxial strain concepts of Darwin, Bashur, and Pecknold (2,4,5), the nonlinear representation of Saenz (12), and the Argyris failure surface (17) in such a way that the relationship correlates well with the best experimental data that the writers were able to find in the literature.

The material model proposed is based on a hypoelastic orthotropic approach. The model is defined in the form of an incremental stress-strain equation in which the material parameters are obtained from stress-"equivalent uniaxial strain" relations.

The paper first presents the assumed form of the incremental-constitutive equations and establishes the shear stiffness in terms of other material constants. A technique for expressing this incremental relationship in terms of incremental

Note.—Discussion open until January 1, 1980. To extend the closing date one month, a written request must be filed with the Editor of Technical Publications, ASCE. This paper is part of the copyrighted Journal of the Engineering Mechanics Division, Proceedings of the American Society of Civil Engineers, Vol. 105, No. EM4, August, 1979. Manuscript was submitted for review for possible publication on September 1, 1978.

[1]Grad. Student, Dept. of Civ. Engrg., Univ. of Alberta, Edmonton, Canada.
[2]Prof. of Civ. Engrg., Univ. of Alberta, Edmonton, Canada.

UNIVERSITY OF ALBERTA LIBRARY

uniaxial strains is then presented, which gives rise to a natural definition of equivalent uniaxial strains. The form of the relationship between equivalent uniaxial strain and stress is then introduced and this becomes the basis from which the incremental elastic moduli are derived in terms of strain parameters. Poisson's ratios are expressed as determined from the experimental data of Kupfer, Hilsdorf, and Rüsch (8). The remaining parameters required for the definition of the incremental properties, i.e., those describing an ultimate stress surface and those describing the corresponding equivalent uniaxial strain surface, are defined. A technique of computer implementation is briefly described. Finally, the predictions of the model are compared with some of the two-dimensional tests of Kupfer, Hilsdorf, and Rüsch (8) and some of the three-dimensional tests of Schickert and Winkler (14).

Form of Incremental Constitutive Relation

The constitutive relation is intended for use in the analysis of axisymmetric structures and, therefore, the constitutive matrix will be 4 × 4. Assuming orthotropy the number of independent material variables is seven, and the matrix, when referred to the orthotropic principal axes, can be written as

$$\begin{Bmatrix} d\epsilon_1 \\ d\epsilon_2 \\ d\epsilon_3 \\ d\gamma_{12} \end{Bmatrix} = \begin{bmatrix} E_1^{-1} & -\nu_{12}E_2^{-1} & -\nu_{13}E_3^{-1} & 0 \\ -\nu_{21}E_1^{-1} & E_2^{-1} & -\nu_{23}E_3^{-1} & 0 \\ -\nu_{31}E_1^{-1} & -\nu_{32}E_2^{-1} & E_3^{-1} & 0 \\ 0 & 0 & 0 & G_{12}^{-1} \end{bmatrix} \begin{Bmatrix} d\sigma_1 \\ d\sigma_2 \\ d\sigma_3 \\ d\tau_{12} \end{Bmatrix} \qquad (1)$$

in which the subscripts 1, 2, and 3 stand for the axes of orthotropy; ϵ and γ = normal and shearing strain, respectively; E and ν = the orthotropic moduli of elasticity and Poisson's ratios, respectively; G = the shear modulus; σ and τ = normal and shearing stress, respectively; and d indicates a differential.

Symmetry gives rise to the following constraints:

$$\nu_{12}E_1 = \nu_{21}E_2 \qquad (2a)$$

$$\nu_{13}E_1 = \nu_{31}E_3 \qquad (2b)$$

$$\nu_{23}E_2 = \nu_{32}E_3 \qquad (2c)$$

Using Eqs. 2 to write Eq. 1 in an explicitly symmetric form yields

$$\begin{Bmatrix} d\epsilon_1 \\ d\epsilon_2 \\ d\epsilon_3 \\ d\gamma_{12} \end{Bmatrix} = \begin{bmatrix} \dfrac{1}{E_1} & \dfrac{-\mu_{12}}{E_1E_2} & \dfrac{-\mu_{13}}{E_1E_3} & 0 \\ & \dfrac{1}{E_2} & \dfrac{-\mu_{23}}{E_2E_3} & 0 \\ & & \dfrac{1}{E_3} & 0 \\ \text{symmetrical} & & & \dfrac{1}{G_{12}} \end{bmatrix} \begin{Bmatrix} d\sigma_1 \\ d\sigma_2 \\ d\sigma_3 \\ d\tau_{12} \end{Bmatrix} \qquad (3)$$

which, upon inversion, becomes

$$\{d\sigma\} = [C]\{d\epsilon\} \quad \text{. . . . .} \quad (4)$$

in which $\{d\sigma\}$ and $\{d\epsilon\}$ = the vectors of incremental stresses and strains appearing in Eq. 3; the constitutive matrix $[C]$ is

$$[C] = \frac{1}{\phi}\begin{bmatrix} E_1(1-\mu_{32}^2) & \sqrt{E_1E_2}\,(\mu_{13}\mu_{32}+\mu_{12}) & \sqrt{E_1E_3}\,(\mu_{12}\mu_{32}+\mu_{13}) & 0 \\ & E_2(1-\mu_{13}^2) & \sqrt{E_2E_3}\,(\mu_{12}\mu_{13}+\mu_{32}) & 0 \\ \text{symmetrical} & & E_3(1-\mu_{12}^2) & 0 \\ & & & G_{12}\phi \end{bmatrix} \quad (5)$$

and $\mu_{12}^2 = \nu_{12}\nu_{21}$ . . . . (6a)

$\mu_{23}^2 = \nu_{23}\nu_{32}$ . . . . (6b)

$\mu_{13}^2 = \nu_{13}\nu_{31}$ . . . . (6c)

$\phi = 1 - \mu_{12}^2 - \mu_{23}^2 - \mu_{13}^2 - 2\mu_{12}\mu_{23}\mu_{13}$ . . . . (6d)

If one now transforms the matrix $[C]$ to a nonorthotropic set of axes $(1',2',3)$ and imposes the requirement that the shear modulus be invariant under this transformation, the result is that

$$G_{12} = \frac{1}{4\phi}\left[E_1 + E_2 - 2\mu_{12}\sqrt{E_1E_2} - (\sqrt{E_1}\,\mu_{23} + \sqrt{E_2}\,\mu_{31})^2\right] \quad \text{. . . . .} \quad (7)$$

Upon specializing Eqs. 3 and 4 to a plane stress condition (by setting $d\sigma_3 = 0$ and removing the third row and column) Eq. 7 reduces to the form obtained by Darwin and Pecknold (4).

Equivalent Uniaxial Strain

With the form of the incremental constitutive relation now defined it remains to describe how the seven incremental hypoelastic moduli are to be determined. The concept of equivalent uniaxial strains, as developed by Darwin and Pecknold (4), which defines the variation of E_1, E_2, and E_3 with respect to the variation of stress, is used herein. The technique may be described as follows.

Let Eq. 4 be written as

$$\begin{Bmatrix} d\sigma_1 \\ d\sigma_2 \\ d\sigma_3 \\ d\tau_{12} \end{Bmatrix} = \begin{bmatrix} E_1B_{11} & E_1B_{12} & E_1B_{13} & 0 \\ E_2B_{21} & E_2B_{22} & E_2B_{23} & 0 \\ E_3B_{31} & E_3B_{32} & E_3B_{33} & 0 \\ 0 & 0 & 0 & G_{12} \end{bmatrix} \begin{Bmatrix} d\epsilon_1 \\ d\epsilon_2 \\ d\epsilon_3 \\ d\gamma_{12} \end{Bmatrix} \quad \text{. . . . .} \quad (8)$$

in which the coefficients B_{ij} can be defined by identifying the matrix terms of Eq. 8 with the corresponding terms in Eq. 5.

Carrying out the multiplication in Eq. 8 yields

$d\sigma_1 = E_1(B_{11}\,d\epsilon_1 + B_{12}\,d\epsilon_2 + B_{13}\,d\epsilon_3)$ . . . . (9a)

$d\sigma_2 = E_2(B_{21}\,d\epsilon_1 + B_{22}\,d\epsilon_2 + B_{23}\,d\epsilon_3)$ . . . . (9b)

$d\sigma_3 = E_3(B_{31}\,d\epsilon_1 + B_{32}\,d\epsilon_2 + B_{33}\,d\epsilon_3)$ . . . . (9c)

UNIVERSITY OF ALBERTA LIBRARY

$$d\tau_{12} = G_{12}\, d\gamma_{12} \quad \text{(9d)}$$

which may be written, in matrix form, as

$$\begin{Bmatrix} d\sigma_1 \\ d\sigma_2 \\ d\sigma_3 \\ d\tau_{12} \end{Bmatrix} = \begin{bmatrix} E_1 & 0 & 0 & 0 \\ 0 & E_2 & 0 & 0 \\ 0 & 0 & E_3 & 0 \\ 0 & 0 & 0 & G_{12} \end{bmatrix} \begin{Bmatrix} d\epsilon_{1u} \\ d\epsilon_{2u} \\ d\epsilon_{3u} \\ d\gamma_{12} \end{Bmatrix} \quad \text{(10)}$$

The vector on the right-hand side of Eq. 10 may be defined as the vector of "equivalent incremental uniaxial strains," whose components are defined in terms of actual incremental strains by identifying with the appropriate terms of Eqs. 9, as

$$d\epsilon_{iu} = B_{i1}\, d\epsilon_1 + B_{i2}\, d\epsilon_2 + B_{i3}\, d\epsilon_3; \quad i = 1, 3 \quad \text{(11)}$$

[Hereinafter the subscripts i and j (only) will be understood to have a range of 3. The summation convention is not used.]

The incremental equivalent uniaxial strains, which can be positive or negative, may be evaluated from Eq. 10 in the simple form

$$d\epsilon_{iu} = \frac{d\sigma_i}{E_i} \quad \text{(12)}$$

and the total equivalent uniaxial strain may be determined by integrating Eq. 12 over the load path to yield

$$\epsilon_{iu} = \int \frac{d\sigma_i}{E_i} \quad \text{(13)}$$

As can be seen from Eq. 3, the incremental uniaxial strain of Eq. 12 is the increment of strain in direction i that the material would exhibit if subjected to a (uniaxial) stress increment $d\sigma_i$ with other stress increments equal to zero. However, $d\epsilon_{iu}$ depends on the current stress ratio, and ϵ_{iu} and $d\epsilon_{iu}$ do not transform in the same manner as stress. Both are fictitious (except in a uniaxial test) and are only significant as a measure on which to base the variation of material parameters.

Eqs. 9*a*, 9*b*, and 9*c* are defined in the material principal axes of orthotropy. If these are assumed to follow the current principal axes of total stress it follows immediately that $d\epsilon_{iu}$ must be defined with respect to the current principal axes of orthotropy. This last statement implies a similarity between equivalent strain parameters in elasto-plastic analyses and equivalent uniaxial strains. Finally, since the ϵ_{iu} are not transformable, they are assumed to be defined only in the current principal stress directions.

The proposed constitutive relationship, based on the concept of equivalent uniaxial strains, can be summarized as

$$d\boldsymbol{\sigma} = \mathbf{F}(d\boldsymbol{\epsilon}, \textstyle\int d\boldsymbol{\sigma}) \quad \text{(14)}$$

in which F implies a functional relationship. This relationship is path-dependent and, while it may not be as rigorous, it bears strong resemblance to the hypoelastic law proposed by Truesdell (16). Thus, some authors (1,15) use the term hypoelastic to describe this as well as similar approaches (3,7,9,10,11,13).

Equivalent Uniaxial Strain-Stress Relation

In the hypoelastic approach developed by Truesdell (16) the stress-strain relationship follows from the incremental constitutive equations. In this case, the stress-strain relationship is problem-dependent. The approach used herein follows that of Darwin and Pecknold (4) and assumes the total stresses to be functions of current equivalent uniaxial strains. This assumption permits the evaluation of the incremental elastic moduli of Eq. 10 in the manner described in the following.

For the purposes of this work, the uniaxial compressive stress-strain relationship of Saenz (12) will be generalized, in a manner similar to that proposed by Bashur and Darwin (2), and used to describe both tensile and compressive response. Writing the Saenz relation in terms of equivalent uniaxial strain yields

$$\sigma_i = \frac{E_0 \epsilon_{iu}}{1 + (R + R_E - 2)\dfrac{\epsilon_{iu}}{\epsilon_{ic}} - (2R - 1)\left(\dfrac{\epsilon_{iu}}{\epsilon_{ic}}\right)^2 + R\left(\dfrac{\epsilon_{iu}}{\epsilon_{ic}}\right)^3} \quad \text{. . . . . (15)}$$

in which the following definitions apply

$$R_E = \frac{E_0}{E_s} \quad \text{. . . . . (16a)}$$

$$E_s = \frac{\sigma_{ic}}{\epsilon_{ic}} \quad \text{. . . . . (16b)}$$

$$R_\sigma = \frac{\sigma_{ic}}{\sigma_{if}} \quad \text{. . . . . (16c)}$$

$$R_\epsilon = \frac{\epsilon_{if}}{\epsilon_{ic}} \quad \text{. . . . . (16d)}$$

$$R = R_E \frac{R_\sigma - 1}{(R_\epsilon - 1)^2} - \frac{1}{R_\epsilon} \quad \text{. . . . . (16e)}$$

The type of curve described by Eq. 15 is shown in Fig. 1, in which the variables appearing in the definitions of Eqs. 15 and 16 are presented. More specifically, E_0 = the initial modulus of elasticity; σ_{ic} = the maximum stress, associated with direction i, that occurs for the current particular principal stress ratio; ϵ_{ic} = the corresponding equivalent uniaxial strain; and σ_{if}, ϵ_{if} = the coordinates of some point on the descending branch of the stress-equivalent strain curve.

Eq. 15 now serves to define the incremental elastic moduli of Eq. 10, for, by Eq. 12

$$E_i = \frac{d\sigma_i}{d\epsilon_{iu}} \quad \text{. . . . . (17)}$$

Differentiating Eq. 15 with respect to ϵ_{iu} yields the right-hand side of Eq. 17 as

UNIVERSITY OF ALBERTA LIBRARY

$$E_i = E_0 \frac{1 + (2R - 1)\left(\frac{\epsilon_{iu}}{\epsilon_{ic}}\right)^2 - 2R\left(\frac{\epsilon_{iu}}{\epsilon_{ic}}\right)^3}{\left[1 + (R + R_E - 2)\frac{\epsilon_{iu}}{\epsilon_{ic}} - (2R - 1)\left(\frac{\epsilon_{iu}}{\epsilon_{ic}}\right)^2 + R\left(\frac{\epsilon_{iu}}{\epsilon_{ic}}\right)^3\right]^2} \quad \ldots \text{(18)}$$

which defines the required moduli.

Poisson's Ratios

The incremental elastic moduli of Eqs. 3 and 10 may be determined from Eq. 18 provided that the parameters shown on Fig. 1 are known for the particular ratio of total stresses. (The evaluation of these parameters will be undertaken subsequently.) However, prior to implementing the incremental stress-strain relationship it is also necessary to determine the values of Poisson's ratio appearing in Eqs. 6. Poisson's ratio was determined from the uniaxial compression data

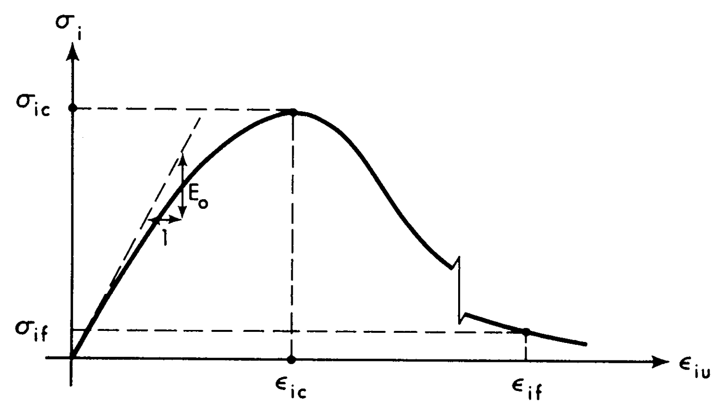

FIG. 1.—Typical Compressive Stress-Equivalent Uniaxial Strain Curve

of the Kupfer, Hilsdorf, and Rüsch tests (8) as a function of strain, by a least-squares fit of a cubic polynomial. This resulted in

$$\nu = \nu_0 \left[1.0 + 1.3763\frac{\epsilon}{\epsilon_{cu}} - 5.3600\left(\frac{\epsilon}{\epsilon_{cu}}\right)^2 + 8.586\left(\frac{\epsilon}{\epsilon_{cu}}\right)^3\right] \quad \ldots\ldots \text{(19a)}$$

$$\text{or} \quad \nu = \nu_0 f\left(\frac{\epsilon}{\epsilon_{cu}}\right) \quad \ldots\ldots \text{(19b)}$$

in which ϵ = the strain in the direction of uniaxial loading; $\epsilon_{cu} = \epsilon_{ic}$ for the uniaxial test; ν_0 = the initial value of ν; and $f(\ )$ is the cubic function displayed in Eq. 19*a*.

It has been assumed that an axially symmetric Poisson's ratio may now be applied to each equivalent uniaxial strain by using Eq. 19*b*. That is, three independent Poisson's ratios are postulated of the form

$$\nu_i = \nu_0 f\left(\frac{\epsilon_{iu}}{\epsilon_{ic}}\right) \qquad (20)$$

Eqs. 6*a*–6*c* may now be written as

$$\mu_{12}^2 = \nu_1 \nu_2 \qquad (21a)$$

$$\mu_{23}^2 = \nu_2 \nu_3 \qquad (21b)$$

$$\mu_{31}^2 = \nu_3 \nu_1 \qquad (21c)$$

The variables appearing in the incremental constitutive matrix of Eq. 3 have, therefore, been completely specified, in terms of ν_0 and the parameters required by Eqs. 16.

Prior to examining the evaluation of the parameters in Eqs. 16, however, it should be noted that the variable ϕ of Eq. 6*d* should always be non-negative. A limiting value of 0.5 has therefore been placed on the values of ν_i determined from Eq. 20. This value corresponds to a limit of zero incremental volume change. Kotsovos and Newmann (6) noted that the point at which this limit is reached corresponds to the onset of "unstable microcrack propagation" that causes the dilatancy phenomenon observed in concrete upon approaching the ultimate strength. It can be argued, however, that dilatancy is observed only when there is a lack of restraint on the geometric deformation of the specimen (see, e.g., Ref. 14) and that placing a maximum limit of 0.5 on Poisson's ratio will yield realistic estimates of stress.

Ultimate Surfaces

The evaluation of the variable moduli defined by Eq. 17 requires the specification of the parameters appearing in the right-hand sides of Eqs. 16. Since these parameters vary with each ratio of stresses, this is most conveniently done by specifying a surface in stress space to define the three values of σ_{ic} for each stress ratio, and a surface in uniaxial strain space to define the three values of ϵ_{ic} that corresponds to these σ_{ic} values (recall Fig. 1).

A surface in stress space that defines the ultimate strengths σ_{ic} for any ratio of stresses is usually called a "failure surface." Because this name is somewhat misleading in the context of a material with strain softening behavior, it is proposed to call such a surface an "ultimate strength surface." The five-parameter surface proposed by Argyris (17), and shown in Fig. 2(*a*), will be used herein to define the ultimate strength surface. The characteristics of this surface are reviewed briefly as follows.

Define the mean normal stress as

$$\sigma_a = \frac{\sigma_1 + \sigma_2 + \sigma_3}{3} \qquad (22)$$

and the mean shear stress as

$$\tau_a = \frac{1}{\sqrt{15}} [(\sigma_1 - \sigma_2)^2 + (\sigma_2 - \sigma_3)^2 + (\sigma_3 - \sigma_1)^2]^{1/2} \qquad (23)$$

Consider the variables σ_a and τ_a to be nondimensionalized by the uniaxial

UNIVERSITY OF ALBERTA LIBRARY

compressive strength, f_{cu}, so that

$$\bar{\sigma}_a = \frac{\sigma_a}{f_{cu}} \quad \ldots\ldots\ldots\ldots\ldots\ldots\ldots\ldots\ldots \text{(2}$$

$$\bar{\tau}_a = \frac{\tau_a}{f_{cu}} \quad \ldots\ldots\ldots\ldots\ldots\ldots\ldots\ldots\ldots \text{(2}$$

The Argyris surface intersects a deviatoric plane (on which σ_a is consta

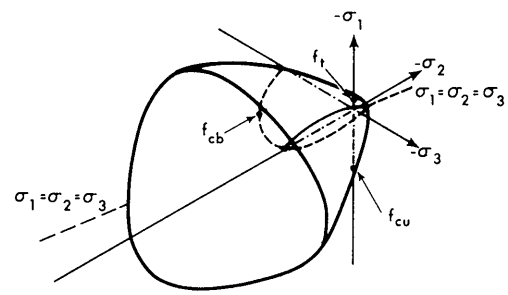

(a) General View of Argyris Failure Surface

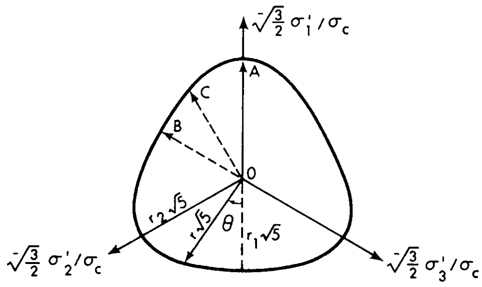

(b) A Deviatoric View of Argyris Surface

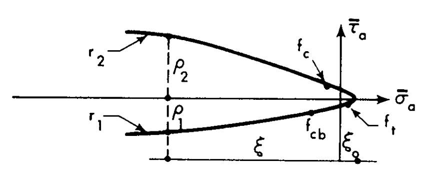

Point	$\bar{\sigma}_a$	$\bar{\tau}_a$
f_c	$-1/3$	$\sqrt{2/15}$
f_t	$\alpha_t/3$	$\alpha_t\sqrt{2/15}$
f_{cb}	$-2\alpha_c/3$	$\alpha_c\sqrt{2/15}$

(c) The Rendulic View of Argyris Surface

FIG. 2.—Argyris Failure Surface

in three symmetric elliptical segments, as indicated in nondimensional stre space in Fig. 2(*b*), in which the deviatoric stress components are indicate as σ_i'. The segments may be described in terms of the variables r and θ, indicate on Fig. 2(*b*), in which r identifies with $\bar{\tau}_a$ defined previously and, because o the symmetries involved, θ may be confined to the range $0 \leq \theta \leq 60°$. Th lues of r at $\theta = 0$, r_1, and at $\theta = 60°$, r_2, are sufficient to define the elliptic rve on any deviatoric plane. For $\sigma_1 \geq \sigma_2 \geq \sigma_3$ then $0 \leq \theta \leq 60°$ and Ref. defines θ and r as

$$s\,\theta = \frac{\sigma_1 + \sigma_2 - 2\,\sigma_3}{\sqrt{2}\ [(\sigma_1 - \sigma_2)^2 + (\sigma_2 - \sigma_3)^2 + (\sigma_3 - \sigma_1)^2]^{1/2}} \qquad (25a)$$

$$= \frac{2\,r_2 r_{21} \cos\theta + r_2(2\,r_1 - r_2)(4\,r_{21}\cos^2\theta + 5\,r_1^2 - 4\,r_1 r_2)^{1/2}}{4\,r_{21}\cos^2\theta + (r_2 - 2\,r_1)^2} \qquad (25b)$$

which $\quad r_{21} = r_2^2 - r_1^2 \qquad (25c)$

point on the surface can then be characterized by

$$= r(\theta, \bar{\sigma}_a) \qquad (25d)$$

The control parameters r_1 and r_2 are assumed to be parabolic functions of e hydrostatic stress and are expressed as

$$= a_0 + a_1\,\bar{\sigma}_a + a_2\,\bar{\sigma}_a^2 \qquad (26a)$$

$$= b_0 + b_1\,\bar{\sigma}_a + b_2\,\bar{\sigma}_a^2 \qquad (26b)$$

he functions r_1 and r_2 are shown in Fig. 2(c) where they are plotted on the -called "rendulic plane."

The values of the coefficients in Eqs. 26 are chosen such that the variables and r_2 pass through a set of control points, as shown in Fig. 2(c). For σ_2 $\sigma_3 - \sigma_1$, then $\theta = 0°$ [Fig. 2(b)] and the points on the surface trace the ariation of r_1 and σ_a varies. This curve must pass through the uniaxial tensile rength point for which $\sigma_2 = \sigma_3 = 0$ and $\sigma_1 = f_t$ (and thus is called the tension branch). It must also pass through the biaxial compression point for hich $\sigma_2 = \sigma_3 = f_{cb}$ and $\sigma_1 = 0$. The nondimensional values of the tensile nd biaxial compression strengths may be defined as

$$= \frac{f_t}{f_{cu}} \qquad (27a)$$

$$= \frac{f_{cb}}{f_{cu}} \qquad (27b)$$

nd their approximate positions on the rendulic plane are indicated in Fig. 2(c). ne additional point on the extension curve is required to define the parabolic ariation of r_1 for Eq. 26a. An arbitrary "high compression" point with $\bar{\sigma}_a$ $= \xi$ may be selected from experimental data to serve this purpose. Let the alue of $\bar{\tau}_a$ at this point be ρ_1, as shown in Fig. 2(c).

To define the variation of r_2 [$\theta = 60°$ on Fig. 2(b)] it is necessary that $= \sigma_3 \geq \sigma_2$. This curve must pass through the uniaxial compression point $= \sigma_3 = 0$, $\sigma_2 = -f_{cu}$ (and thus is called the compression branch). It is so required to intersect the hydrostatic curve on the rendulic plane at the me location as the r_1 curve ($\bar{\sigma}_a = \xi_0$), and to pass through the experimental oint (ξ, ρ_2) for which ρ_2 is determined in the same manner as ρ_1.

The values of the coefficients in Eqs. 26 can be determined from the five ontrol points described previously. Expressions for these coefficients are given

UNIVERSITY OF ALBERTA LIBRARY

in Appendix I (17). The Argyris surface is therefore completely defined serves to evaluate the three σ_{ic} values required in Eqs. 16 for any ratio stresses.

However, Eqs. 16 also require the evaluation of the equivalent uniaxial stra ϵ_{ic}, associated with the ultimate strength points, σ_{ic}. For this purpose i postulated that there is a surface in equivalent uniaxial strain space that the same form as the Argyris stress surface. It should be remembered t except for uniaxial stress paths, equivalent uniaxial strains are hypothet

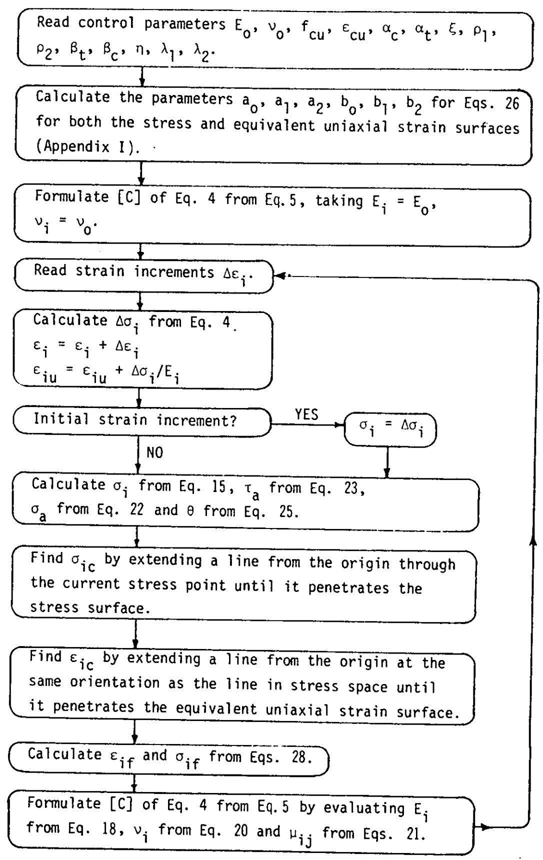

FIG. 3.—Flow Chart for Implementation of Constitutive Equations

quantities. However, we define the analogous strain quantities ϵ_a^* and γ_a^* correspond with σ_a and τ_a, respectively, by replacing σ_1, σ_2, and σ_3 in Eq 22–23 by ϵ_{1u}, ϵ_{2u}, and ϵ_{3u}, respectively, where the * in the notation impl equivalent uniaxial strain quantities. The analagous nondimensionalization Eqs. 24 is carried out with ϵ_{cu}, the strain corresponding to the uniaxial compressi strength, replacing f_{cu} in order to determine $\bar{\epsilon}_a^*$ and $\bar{\gamma}_a^*$. Analogous quantiti for the strain control points described in association with the stress surfa follow directly and Eqs. 25 and 26, together with the equations of Append which may also be used directly with the appropriate changes of variables. lote, however, that uniaxial strains are available from tests only for the control oints corresponding to f_t and f_{cu}. Equivalent uniaxial strains at the other three ontrol points are fictitious strains that cannot be observed directly. These points ave been determined, herein, by trial and error until reasonable strain correpondence was obtained.

The remaining parameters required by Eqs. 16 are the values of σ_{if} and ϵ_{if} n the descending branch of the stress-equivalent uniaxial strain curve (Fig.

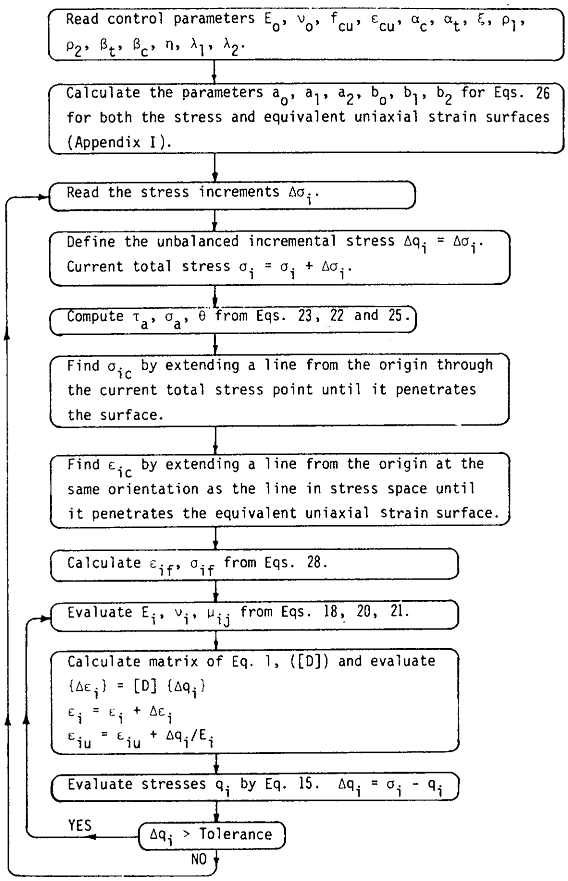

FIG. 4.—Flow Chart for Constitutive Relation to Follow Specified Stress Path

). The definition of these points is not possible on any rigorous experimental asis since the descending branch of the stress-strain curve is highly test-dependent nd is generally unavailable from statically determinate tests. This portion of he curve must usually be inferred from the behavior of flexural stress distribuions. The following assumptions will be adopted:

$$_{if} = 4\,\epsilon_{ic} \quad \ldots\ldots \quad (28a)$$

OF ALBERTA LIBRARY

$$\sigma_{if} = \frac{\sigma_{ic}}{4} \quad \ldots\ldots\ldots\ldots\ldots\ldots\ldots\ldots\ldots\ldots$$

The description of the determination of all the material variables req[uired] for the implementation of the constitutive relationship is now complete. [N]... that, although the development has been carried out in the context of

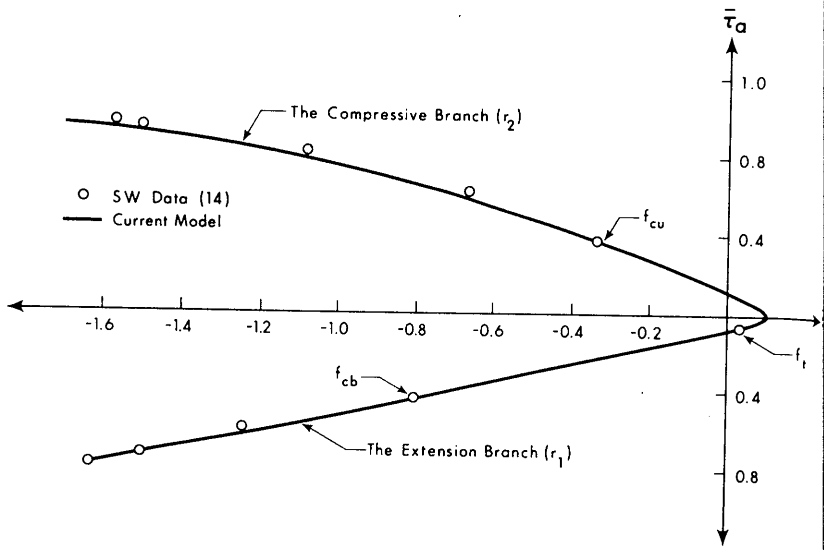

FIG. 5.—Comparison of Curves on Rendulic Plane with Schickert-Winkler Data (

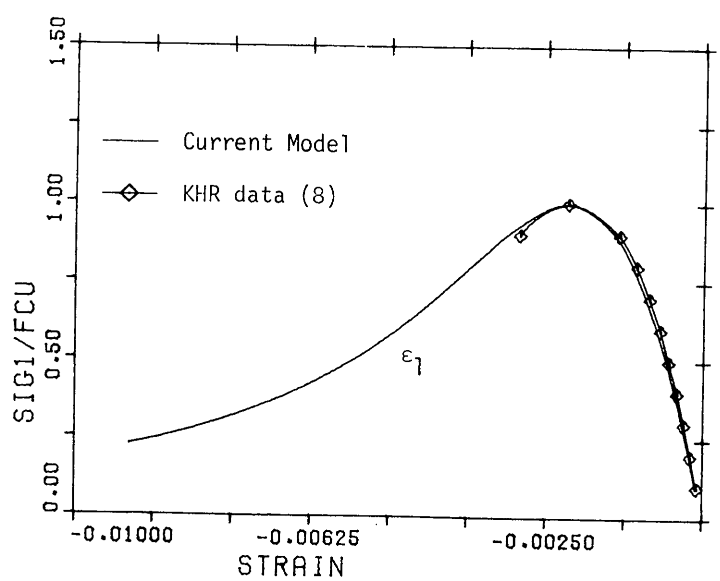

FIG. 6.—Strains for Uniaxial Compression

isymmetric relation, the extension of the technique to the general three-dimen-
nal context is trivial, since this only requires the definition of the additional
cremental shear moduli G_{23} and G_{31} that can be determined in the same manner
G_{12} (see Eqs. 7, 20, and 21).

PLEMENTATION

The technique of implementing the constitutive relationship is described herein
the context of its usage in an iterative nonlinear finite element program.
such an application, strain increments are imposed and it is required to
nd the associated stress increments. A flow chart for this application is shown
Fig. 3. The strain input parameters β_c, β_t, η, λ_1, and λ_2, appearing in

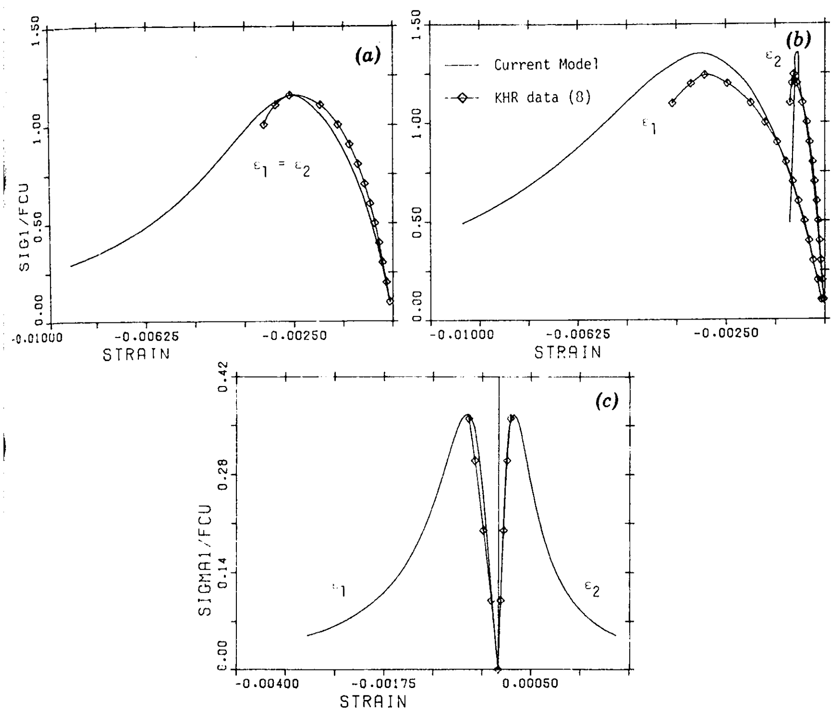

FIG. 7.—Strains for Biaxial Stress Ratio: (*a*) −1:−1; (*b*) −1:−0.52; (*c*) −1:0.204

ig. 3, have not previously been defined but are analogous to the stress input
arameters α_c, α_t, ξ, ρ_1, and ρ_2, respectively, defined in the preceding section.
Although Fig. 3 is the normal type of application, it is useful in comparing
with experimental results to be able to determine the strains associated with
predefined stress path. A flow chart for this type of application, which requires
teration, is shown in Fig. 4.

ERIFICATION OF MODEL

If the three-dimensional constitutive relationship described herein has validity
t should be able to predict strains associated with test results in the literature.

OF ALBERTA LIBRARY

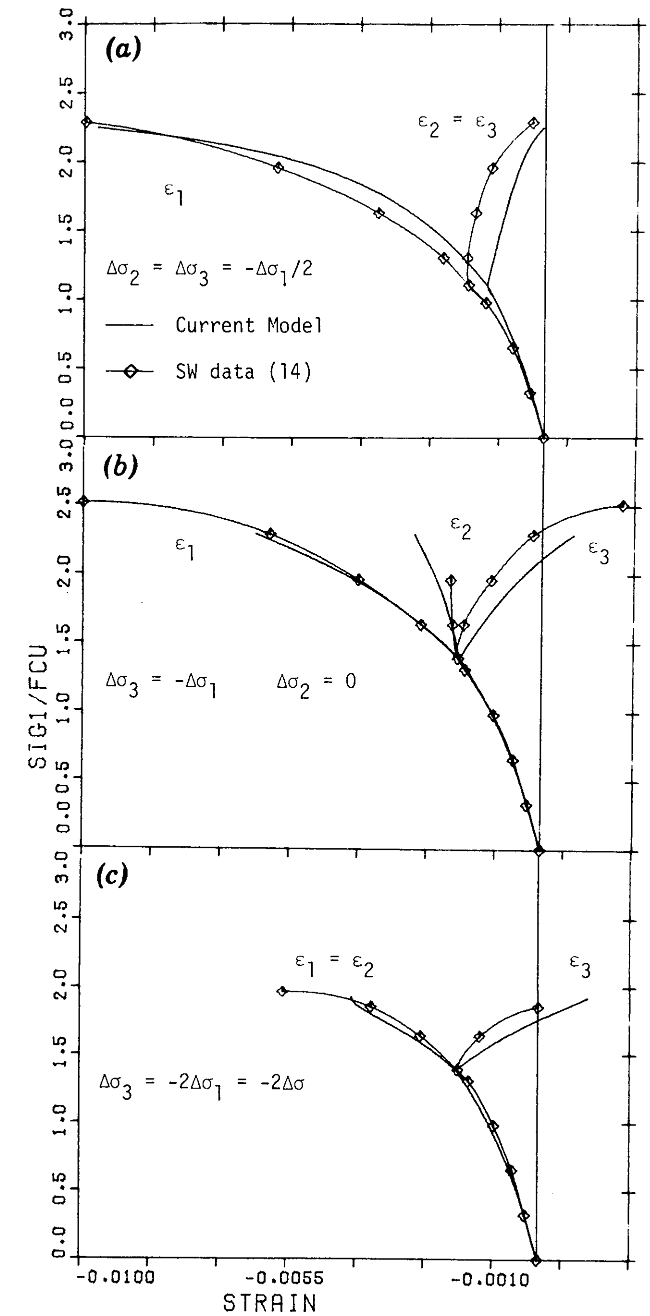

FIG. 8.—Strains for Triaxial Stress Changes: (*a*) −1:0.5:0.5; (*b*) −1:0:1; (*c*) 0.5:0.5:−1

he parameters of Eqs. 26 have been evaluated for control points of the chickert-Winkler data (14). The correspondence of these equations on the ndulic plane with the data of Schickert and Winkler is shown in Fig. 5. The alues of r_1 and r_2 are seen to agree suitably with this data set. We now consider ress-strain comparisons with two sets of experimental data.

A comparison of predicted strains with selected sets of measurements by upfer, Hilsdorf, and Rüsch (8), hereinafter referred to as the KHR data, in series of two-dimensional tests is shown in Figs. 6 and 7. The parameters hat have been used to model this material are given in Appendix II. Fig. 6 hows the uniaxial compression comparison, and Fig. 7(a) shows the biaxial ompression comparison. Since the peak stresses and corresponding strains are ontrol points on the surfaces, exact correlation is obtained at these points. ig. 7(b) shows the comparison for biaxial compression in the ratio of $-1{:}-0.52$. ince the five-parameter three-dimensional Argyris ultimate strength surface oes not predict the same strength as the KHR two-dimensional failure surface, here is a discrepancy of approx 8% in this instance. A comparison of typical esponse in the tension-compression zone is shown in Fig. 7(c).

The preceding comparisons are those of the three-dimensional theory with lane stress tests. A comparison of the theory with some of the three-dimensional ests of Schickert and Winkler (14), hereinafter referred to as the SW data, s shown in Fig. 8. These tests were carried out by loading along a hydrostatic tress path with deviatoric stress equal to zero, and then incrementing the three rincipal stresses in such a way that the hydrostatic stress remained constant while the deviatoric stress varied. Fig. 8(a) shows results for a deviatoric stress path along line O-A of Fig. 2(b) ($\theta = 60°$). Fig. 8(b) shows results for a deviatoric tress path along line O-C of Fig. 2(b) ($\theta = 30°$). Fig. 8(c) shows results for deviatoric stress path along line O-B of Fig. 2(b) ($\theta = 0°$).

It can be seen that the model gives a reasonable simulation of the SW experimental stress-strain response along each of these nontrivial stress paths.

ONCLUSIONS

A three-dimensional constitutive relationship, developed from the concepts dvanced by Darwin, et al. (2, 4, and 5), Saenz (12), and William, et al. (17), as been proposed. A comparison of the proposed theory with two sets of xperimental data indicates that it can give reasonable results, for both tensile nd compressive response, and therefore should be suitable for inclusion in ny finite element program for the nonlinear analysis of reinforced concrete tructures.

CKNOWLEDGMENTS

The research upon which this paper is based was carried out during the course of studies of the first writer in partial fulfillment of the requirements for the degree of Doctor of Philosophy in Civil Engineering at the University of Alberta. This work was supported by the Killam Foundation, the Computing Centre of the University of Alberta, the National Research Council of Canada, and he Atomic Energy Control Board of Canada.

UNIVERSITY OF ALBERTA LIBRARY

Appendix I.—Formulas for Coefficients of Eqs. 26

The coefficients of Eqs. 26 are determined from the following formulas (1

$$\frac{a_2}{9}=\frac{\sqrt{1.2}\,\xi(\alpha_t-\alpha_c)-\sqrt{1.2}\,\alpha_t\alpha_c+\rho_1(2\alpha_c+\alpha_t)}{(2\alpha_c+\alpha_t)(3\xi-2\alpha_c)(3\xi+\alpha_t)}$$

$$a_1=\frac{1}{3}(2\alpha_c-\alpha_t)\,a_2+\frac{\sqrt{1.2}\,(\alpha_t-\alpha_c)}{2\alpha_c+\alpha_t}$$

$$a_0=\frac{2}{3}\alpha_c a_1-\frac{4}{9}\alpha_c^2 a_2+\sqrt{\frac{2}{15}}\,\alpha_c$$

$$\xi_0=\frac{-a_1-\sqrt{a_1^2-4a_0a_2}}{2a_2}$$

$$\frac{b_2}{9}=\frac{\rho_2\left(\xi_0+\frac{1}{3}\right)-\sqrt{\frac{2}{15}}\,(\xi_0+\xi)}{(\xi+\xi_0)(3\xi-1)(3\xi_0+1)}$$

$$b_1=\left(\xi+\frac{1}{3}\right)b_2+\frac{\sqrt{1.2}-3\rho_2}{3\xi-1}$$

$$b_0=-\xi_0 b_1-\xi_0^2 b_2$$

in which the variables are defined in the body of the paper.

Appendix II.—Parameters for Concrete Models

The strength parameters for KHR data (8) are: $f_{cu}=-4{,}650$ psi; $\alpha_c=1.1$ $\alpha_t=0.091$; $r_1=0.048835-0.513326\,(\bar{\sigma}_a)-0.038292\,(\bar{\sigma}_a)^2$; and $r_2=0.08796$ $-\,0.909151\,(\bar{\sigma}_a)-0.232785\,(\bar{\sigma}_a)^2$.

The deformation parameters for KHR data (8) are: $\epsilon_{cu}=-0.00215$; $\beta_c=$ 1.7512; $\beta_t=0.0461$; $\nu_0=0.195$; $E_0=4{,}700{,}000$ psi; $r_1=0.025115-0.53880$ $(\bar{\epsilon}_a^*)-0.010786\,(\bar{\epsilon}_a^*)^2$; and $r_2=0.048340-1.027311\,(\bar{\epsilon}_a^*)-0.230689\,(\bar{\epsilon}_a^*)^2$.

The strength parameters for Schickert-Winkler data (14) are: $f_{cu}=-4{,}43$ psi; $\alpha_c=1.21$; $\alpha_t=0.1$; $r_1=0.053627-0.512079\,(\bar{\sigma}_a)-0.038226\,(\bar{\sigma}_a)^2$; and $r_2=0.095248-0.891175\,(\bar{\sigma}_a)-0.244420\,(\bar{\sigma}_a)^2$.

The deformation parameters for Schickert-Winkler data (14) are: $\epsilon_{cu}=$ -0.00283; $\beta_c=1.3$; $\beta_t=0.0461$; $\nu_0=0.18$; $E_0=3{,}800{,}000$ psi; $r_1=0.02507$ $-\,0.539616\,(\bar{\epsilon}_a^*)-0.024032\,(\bar{\epsilon}_a^*)^2$; and $r_2=0.045268-0.974103\,(\bar{\epsilon}_a^*)-0.04338$ $(\bar{\epsilon}_a^*)^2$.

Appendix III.—References

1. Argyris, J. H., Krempl, E., and William, K. J., "Constitutive Models and Finite Element Solution of Inelastic Behavior," presented at the August 9–13, 1976, United States-German Symposium on "Formulations and Computational Algorithms in Finite Element Analysis," held at the Massachusetts Institute of Technology, Boston, Mass.
2. Bashur, F. K., and Darwin, D., "Nonlinear Biaxial Law for Concrete," *Journal*

of the Structural Division, ASCE, Vol. 104, No. ST1, Proc. Paper 13495, Jan., 1978, pp. 157–170.
3. Coon, M. D., and Evans, R. J., "Incremental Constitutive Laws and their Associated Failure Criteria with Application to Plain Concrete," *International Journal of Solids and Structures*, Vol. 8, 1972, pp. 1169–1180.
4. Darwin, D., and Pecknold, D. A., "Analysis of Cyclic Loading of Plane R/C Structures," *Computers and Structures*, Vol. 7, Pergamon Press, Inc., New York, N.Y., 1977, pp. 137–147.
5. Darwin, D., and Pecknold, D. A., "Nonlinear Biaxial Law for Concrete," *Journal of the Engineering Mechanics Division*, ASCE, Vol. 103, No. EM2, Proc. Paper 12839, Apr., 1977, pp. 229–241.
6. Kotsovos, M. D., and Newman, J. B., "Behavior of Concrete Under Multiaxial Stress," *American Concrete Institute Journal, Proceedings*, Vol. 74, No. 9, Sept., 1977, pp. 443–446.
7. Kupfer, H. B., and Gerstle, K. H., "Behavior of Concrete under Biaxial Stresses," *Journal of the Engineering Mechanics Division*, ASCE, Vol. 99, No. EM4, Proc. Paper 9917, Aug., 1973, pp. 853–866.
8. Kupfer, H. B., Hilsdorf, H. K., and Rüsch, H., "Behavior of Concrete under Biaxial Stresses," *American Concrete Institute Journal, Proceedings*, Vol. 66, No. 8, Aug., 1969, pp. 656–666.
9. Link, J., "Eine Formulierung des zweiaxialen Verformungs-und Bruchverhaltens von Beton," *Deutscher Asschuss für Stahlbeton*, Heft 270, Berlin, West Germany, 1976.
10. Liu, T. C. Y., Nilson, A. H., and Slate, F. O., "Biaxial Stress-Strain Relations for Concrete," *Journal of the Structural Division*, ASCE, Vol. 98, No. ST5, Proc. Paper 8905, May, 1972, pp. 1025–1034.
11. Romstad, K. M., Taylor M. A., and Herrmann, L. R., "Numerical Biaxial Characterization for Concrete," *Journal of the Engineering Mechanics Division*, ASCE, Vol. 100, No. EM3, Proc. Paper 10879, Oct., 1974, pp. 935–948.
12. Saenz, I. P., discussion of "Equation for the Stress-Strain Curve of Concrete," by P. Desayi and S. Krishnan, *American Concrete Institute Journal, Proceedings*, Vol. 61, No. 9, Sept., 1964, pp. 1229–1235.
13. Sarne, Y., "Material Nonlinear Time Dependent Three-Dimensional Finite Element Analysis of Reinforced and Prestressed Concrete Structures," thesis presented to the Massachusetts Institute of Technology, at Cambridge, Mass., in 1974, in partial fulfillment of the requirements for the degree of Doctor of Philosophy.
14. Schickert, G., and Winkler, H., "Results of Test Concerning Strength and Strain of Concrete Subjected to Multiaxial Compressive Stresses," *Deutscher Ausschuss für Stahlbeton*, Heft 277, Berlin, West Germany, 1977.
15. Schnobrich, W. C., "Behavior of Reinforced Concrete Structures Predicted by the Finite Element Method," *Computers and Structures*, Vol. 7, Pergamon Press, Inc., New York, N.Y., 1977, pp. 365–376.
16. Truesdell, C., "Hypo-elasticity," *Journal of Rational Mechanics Analysis*, Vol. 4, 1955, pp. 83–133.
17. William, K. J., and Warnke, E. P., "Constitutive Model for the Triaxial Behavior of Concrete," *International Association for Bridge and Structural Engineering Proceedings*, Vol. 19, 1975.

UNIVERSITY OF ALBERTA LIBRARY

Appendix IV.—Notation

The following symbols are used in this paper:

a_0, a_1, a_2 = coefficients of Eq. 26;
B_{ij} = coefficients in Eqs. 9 and 11;
b_0, b_1, b_2 = coefficients of Eq. 26;
$[C], C_{ij}$ = stiffness coefficients in incremental constitutive relation (Eqs. 4 and 5);
E_i = orthotropic strain-dependent elastic modulus in direction i;

E_0 = initial modulus of elasticity;
E_s = pseudo-secant modulus of elasticity at peak stress;
F, f = indicate functions (Eqs. 14 and 19);
f_{cb} = ultimate strength in biaxial compression;
f_{cu} = ultimate strength in uniaxial compression;
f_t = ultimate strength in uniaxial tension;
G_{ij} = shear moduli;
i, j = indices with range of three;
R = ratio of Eq. 16;
R_E = ratio of moduli E_0/E_s (Eq. 16*a*);
R_ϵ = ratio of strains $\epsilon_{if}/\epsilon_{ic}$ (Eq. 6*d*);
R_σ = ratio of stresses σ_{ic}/σ_{if} (Eq. 16*c*);
r = nondimensional mean shear stress on deviatoric plane [Fig. 2(*b*)];
r_1, r_2 = nondimensional control parameters on deviatoric plane [(Fig. 2(*b*)];
r_{21} = $r_2^2 - r_1^2$;
u = subscript indicating equivalent uniaxial quantity;
α_c = nondimensionalized biaxial compressive strength (Eq. 27*b*);
α_t = nondimensionalized uniaxial tensile strength (Eq. 27*a*);
β_c = nondimensionalized equivalent uniaxial strain at stress point (f_{cb}, f_{cb}, 0);
β_t = nondimensionalized uniaxial strain at stress point (f_t, 0, 0);
γ_{ij} = shear strain;
$\gamma_a^*, \bar{\gamma}_a^*$ = equivalent uniaxial mean shear strain and its nondimensionalized value with respect to ϵ_{cu};
ϵ = normal strain;
$\epsilon_a^*, \bar{\epsilon}_a^*$ = equivalent uniaxial mean normal strain and its nondimensionalized value with respect to ϵ_{cu};
ϵ_{cu} = uniaxial compressive strain at stress point (f_{cu}, 0, 0);
ϵ_i = real strain in direction i;
ϵ_{ic} = equivalent uniaxial peak strain in direction i for multiaxial stress condition (Fig. 1);
ϵ_{if} = equivalent uniaxial strain in direction i for stress σ_{if} for multiaxial stress condition (Fig. 1);
ϵ_{iu} = equivalent uniaxial strain in direction i (Fig. 1);
η = control point for equivalent uniaxial mean strain on rendulic strain plane;
θ = orientation of stress point on deviatoric plane [Fig. 2(*b*)];
λ_1, λ_2 = values of $\bar{\gamma}_a^*$ at mean strain η for extension branch on rendulic strain plane;
μ_{ij} = equivalent Poisson's ratios (Eqs. 6 and 21);
ν = Poisson's ratio;
ν_i = Poisson's ratio axially symmetric about axis i;
ν_{ij} = Poisson's ratios, Eqs. 1 and 2;
ν_0 = initial value of Poisson's ratios;
ξ = control value of nondimensionalized mean normal stress;
ξ_0 = nondimensionalized mean normal stress at zero value of $\bar{\tau}_a$ [Fig. 2(*c*)];
ρ_1, ρ_2 = values of $\bar{\tau}_a$ for $\bar{\sigma}_a = \xi$ on rendulic plane;

$\sigma_a, \bar{\sigma}_a$ = mean normal stress and its nondimensionalized value with respect to f_{cu} (Eqs. 22 and 24);
σ_i = normal stress in direction i;
σ_{ic} = peak stress in direction i for multiaxial stress condition (Fig. 1);
σ_{if} = stress for equivalent uniaxial strain ϵ_{if} for multiaxial stress condition (Fig. 1);
σ_i' = deviatoric principal stress;
$\tau_a, \bar{\tau}_a$ = mean shear stress and its nondimensionalized value with respect to f_{cu} (Eqs. 23 and 24b);
τ_{ij} = shear stress; and
ϕ = factor defined in Eq. 6d.

OF ALBERTA LIBRARY

View publication stats